

Cloning and Characterization of a Myosin from Characean Alga, the Fastest Motor Protein in the World¹

Taku Kashiya^{*}, Naohiro Kimura[†], Tetsuro Mimura[‡] and Keiichi Yamamoto^{*2}

^{*}Department of Biology, Chiba University, Yayoicho, Inage-ku, Chiba 263-8522; [†]Department of Bioengineering, Soka University, Tangicho, Hachioji, Tokyo 192-8577; and [‡]Department of Biology, Hitotsubashi University Kunitachi, Tokyo 186-8601

Received March 9, 2000; accepted March 28, 2000

In characean algae, very rapid cytoplasmic streaming is generated by sliding movement of an unconventional myosin on fixed actin cables. The speed of this sliding movement is the fastest among many molecular motors known so far. We have cloned a set of overlapping cDNAs encoding the heavy chain of this myosin by immunoscreening with antibody raised against characean myosin. The molecular mass of this heavy chain is 248 kDa, and the protein has a conserved motor domain, six IQ motifs, an extensive α -helical coiled-coil domain, and a C-terminal globular domain. Phylogenetic analysis suggested that this myosin belongs to class XI.

Key words: characean alga, cloning, cytoplasmic streaming, motor protein, myosin.

Cytoplasmic streaming in characean algae is known to be extremely fast (about 70 $\mu\text{m/s}$ at 20°C). It is generated by an unconventional myosin which, bound to endoplasmic reticulum, runs on the track of actin bundles attached to chloroplasts lying under the plasma membrane (1, 2). We purified this unique myosin from *Chara corallina* (3). The myosin can translocate fluorescently labeled F-actin at a velocity of about 50 $\mu\text{m/s}$ in the *in vitro* motility assay. This sliding velocity is about 10 times higher than that of muscle myosin and is the highest of all achieved not only by myosins but also by other motor proteins. Electron microscopic study revealed that this myosin has two heads with similar size and shape to those of muscle myosin. But its tail is shorter than that of muscle myosin and it has a globular structure at the distal end, which is probably the site of interaction with the membrane (4). The actin-activated Mg-ATPase activity of characean myosin is not higher than that of muscle myosin. Since the head size and the turnover rate of this myosin are not so different from those of muscle myosin, its high velocity may be accomplished by rapid conformational change during the power stroke. Therefore, determination of its primary structure and comparison with that of muscle myosin are essential to understand why this myosin can support such fast movement of actin filaments. In this study, we cloned a set of overlapping cDNAs encoding the full-length amino acid sequence of this myosin. The structure predicted from its amino acid sequence agreed well with that observed previously by electron microscopy. Several interesting differences and similarities in sequence were found between this myosin and muscle myosin.

MATERIALS AND METHODS

Cloning—Total RNA of *C. corallina* was obtained by a procedure combining the acid guanidinium-phenol-chloroform (AGPC) method for animal cells and the cetyltrimethylammonium bromide (CTAB) method for plant cells. Poly(A)⁺ RNA was isolated from total RNA using an oligo-dT column [poly(A)⁺ RNA purification kit, Pharmacia] according to the manufacturer's instructions. Double-stranded cDNA was synthesized with both random and oligo-dT primer from poly(A)⁺ RNA using SuperScript™ Choice System for cDNA Synthesis (Gibco BRL), and ligated into λ ZAP II expression vector (Stratagene). Then the vector was packaged *in vitro* using a Gigapack III Gold Packaging Extract (Stratagene) according to the manufacturer's instructions.

The initial set of characean myosin cDNA clones was immunoscreened from a *C. corallina* cDNA library with a polyclonal antibody raised in rabbit against characean myosin (3). Immunoscreening was done according to standard procedure. Membranes were incubated with primary antibody, and alkaline phosphatase-conjugated goat anti-rabbit IgG (Promega) was used to detect positive plaques. Nucleotide sequencing was carried out by the dideoxy chain termination method (5) using Thermo Sequenase (Amersham) and a DNA sequencer (ALF Express DNA sequencer, Pharmacia). Alignment of nucleotide sequences and comparison were performed by use of GENETYX-MAC Ver. 8 (Software Development). Databank searching was carried out using the BLAST program in the DDBJ (DNA Data Bank of Japan). Predictions for coiled-coil structure were carried out using the COILS Ver. 2.2 (6, 7). Two overlapping clones (106 and 107) were isolated from 600,000 phage plaques by immunoscreening using polyclonal antibody against characean myosin. These clones contained single open reading frame, which encodes the C-terminal region of *C. corallina* myosin (CCM), and the complete 3' noncoding sequence with poly(A) tail. The BLAST search suggested that the C-terminal sequence had some homology to those of class V

¹ This work was supported by a Grant-in-Aid for Scientific Research and a Grant-in-Aid for Scientific Research on Priority Areas from The Ministry of Education, Science, Sports and Culture of Japan.

² To whom correspondence should be addressed. Phone/Fax: +81-43-290-2809, E-mail: yamamoto@bio.s.chiba-u.ac.jp

and XI myosins. To extend sequences obtained by immunoscreening in the 5' direction rapidly, degenerated PCR was performed. In view of the similarity between the obtained cDNA and class V and XI myosins, degenerated primer LDIY-5' (5'-YTNGAYATHTAYGGNTTYGA-3') encoding amino acid sequence LDIYGFE, which is conserved among class V and XI myosins, and gene-specific primer CCM-3' (5'-TGCCTCCCTCTATCCTTTTCGCAGA-3') were synthesized. PCR product was subcloned into pBluescript II plasmid (Stratagene) by TA cloning. *IQ* (1,692 bp) clone was obtained by this procedure. DNA sequence of the PCR product was identical to that of *106* in the overlapping region. To obtain the complete sequence, the *Pst*I fragment of *IQ* was used as a probe to screen the same library. Hybridization and detection were carried out using DIG DNA labeling and detection kit (Boehringer Mannheim). The positive recombinant phage was subjected to *in vivo* excision to yield pBluescript phagemid using the ExAssist™/SOLR™ system (Stratagene). Two clones *λQ1* and *AT2* were obtained by this procedure. These overlapping clones contained both 5' and 3' noncoding sequences and a long open reading frame of 2,182 amino acids with a calculated molecular mass of 247 723 (accession number: AB007459).

Expression of Fusion Protein and Antibody Production—DNA fragments encoding distinct domains of characean myosin heavy chain were obtained by digesting with appropriate restriction enzymes, subcloned into pRSET expression vector (Invitrogen), and expressed in *Escherichia coli* BL21. Peptides in the cells were separated from other proteins by SDS-PAGE. These peptides in the gel slices were collected electrophoretically and injected into rabbit.

Immunoblotting—Frozen, ground, and dried *C. corallina* was dissolved in SDS solution. This characean whole sample was subjected to electrophoresis on 10% SDS-polyacrylamide gel. Proteins in the gel were transferred to nitrocellulose membrane and immunoblotted according to standard procedure. The primary antibody was allowed to react

for 1 h and its location was detected by alkaline phosphatase-conjugated goat anti-rabbit IgG (1:5,000 dilution, Promega).

Phylogenetic Analysis—Multiple alignment was performed and an unrooted phylogenetic tree was created based on the neighbor-joining method using the program in Clustal X (8). Bootstrap resampling (1,000 trials) was used to estimate the degree of confidence in the branching order.

Inhibition of Motile Activity by Antibody—The effect of antibody on the motile activity of characean myosin was studied as follows. Crude extract of characean cytoplasm was briefly centrifuged to remove chloroplasts and loaded into a flow cell (3). After incubation with blocking solution containing 0.5 mg/ml BSA, characean myosin adsorbed on the cover slip was treated with either anti-myosin head IgG or control nonimmune IgG for 15 min at room temperature. *In vitro* motility assay was performed as described previously (3).

RESULTS

Domain Structure of the Characean Myosin—Amino acid sequence analysis revealed that the *C. corallina* myosin (CCM) was composed of a head domain, a neck domain, a coiled-coil rod domain, and a globular tail domain (Fig. 1). Comparison of the amino acid sequence of CCM with those of other myosins revealed that *Arabidopsis* MYA1 (9) has the most closely related sequence. The head domain (amino acids 1 to 740) shared 62.8% sequence identity with that of MYA1. Although the whole domain structure was similar to that of class V myosin from chicken (P190) (10), sequence identity with the head domain of P190 was lower than that with MYA1 (Fig. 1). Several sequence motifs conserved in the head domain of all myosins were also seen in CCM (Fig. 2). These are a loop around a phosphate group (P-loop), switch I, switch II, and a helix following switch II. Highly reactive cysteine residues known as SH₁ and SH₂

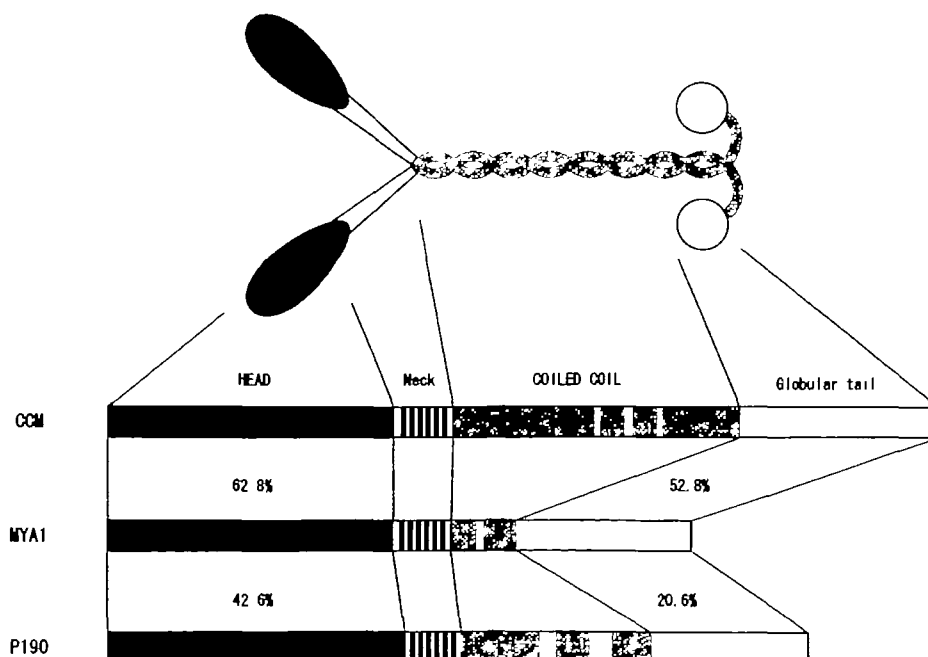


Fig. 1. Structure of *Chara corallina* myosin (CCM) deduced from its amino acid sequence, and homology of the sequence to those of type XI myosin (MYA1, accession number Z28389) and type V myosin (p190, accession number Z11718). Regions predicted to form a coiled-coil structure with probability of more than 90% are shaded. The percent amino acid identity of the head and globular tail domains as compared to CCM is indicated.

are also found in the corresponding location.

The neck domain of CCM (amino acids 741 to 883) had six imperfect tandem repeats of the 23–25 amino acid sequence referred to as the IQ motif. These are probably sites for light chain binding. Directly following the neck region was a region (amino acids 884 to 1635) predicted to form an extensive coiled-coil structure. In particular, the region between residues 1073 to 1635 was composed of highly conserved 33aa tandem repeats (3 to 5 times), which are predicted to form the coiled-coil structure. These four repeats were separated at three regions by another 33 aa motif that is predicted to break coiled-coil structure.

The distal C-terminal sequence (amino acids 1636 to 2182) of CCM shared 52.8% sequence identity with that of MYA1 (Fig. 1). Like those of class V and XI myosins, this region was predicted to form a globular structure. This

region also contained a motif conserved in these classes of myosins (9, 10).

Phylogenetic Analysis—Recent phylogenetic analysis using myosin head sequence indicated that the myosin molecules sequenced to date could be classified into at least 13 distinct classes (11). The same analysis was performed including sequence data of CCM. The resulting phylogenetic tree is shown in Fig. 3. A bootstrap value of 1,000 at the node that joins the higher plant Class XI myosins (MYA1, MYA2 *etc.*) and CCM strongly supports the idea that CCM can be classified as a Class XI myosin.

Immunochemical Analysis of CCM—Antibodies raised against the coiled-coil region (amino acids 1050 to 1642) and the globular tailpiece (amino acids 1639 to 2182) were used. Immunoblot analysis showed that these antibodies recognized the same protein band out of whole characean

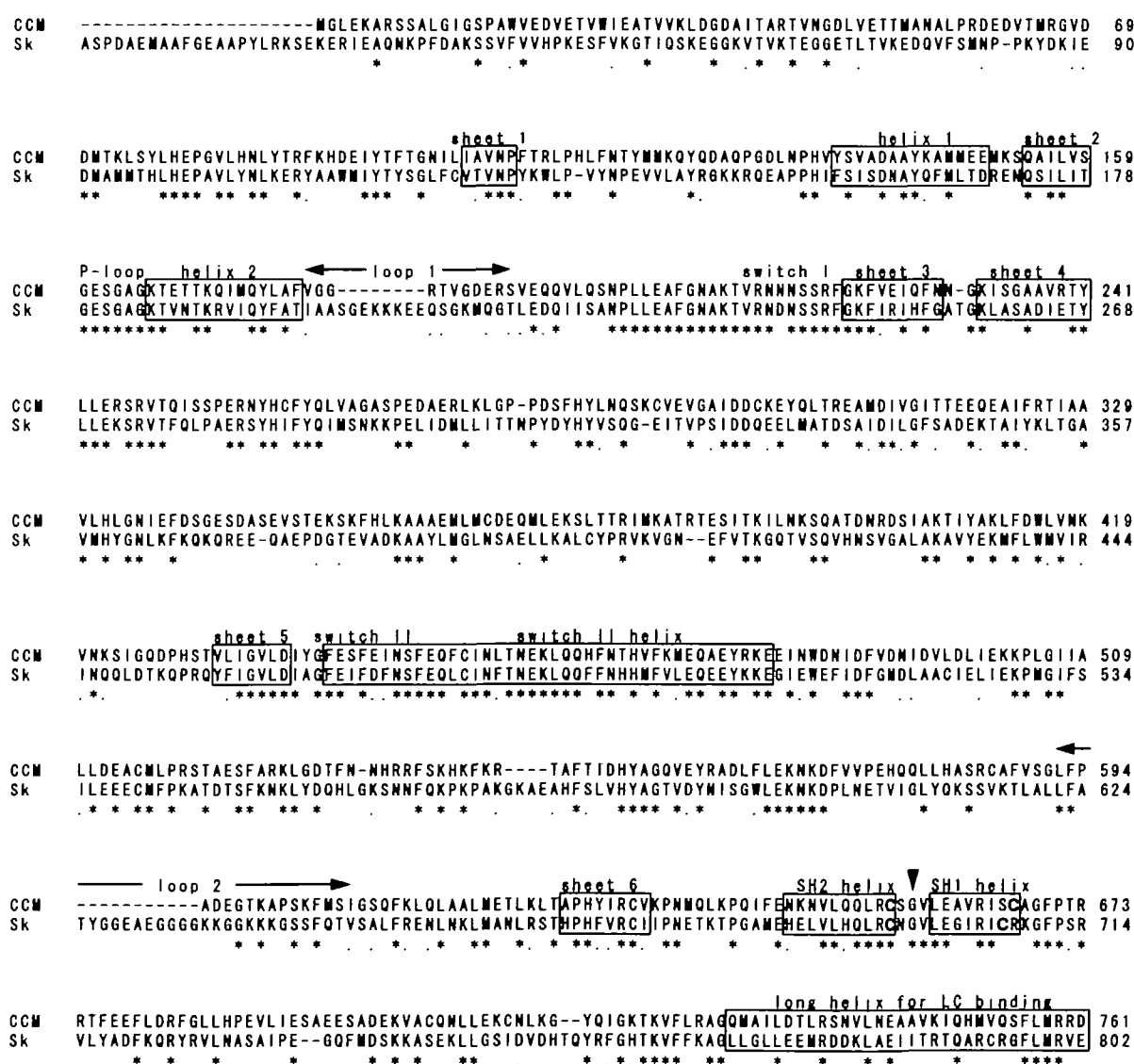


Fig. 2. Comparison of the primary structure of the head domain of *Chara corallina* myosin (CCM, upper sequence) with that of chicken skeletal muscle myosin (Sk, lower sequence). Identical and similar residues are indicated by asterisks and periods, respectively. Characteristic sequence motifs are boxed. Reactive cysteine residues (SH₁ and SH₂) of skeletal muscle myosin and corre-

sponding residues of CCM are indicated by bold typeface. The arrowhead between SH₁ and SH₂ denotes a glycine residue, which is the putative pivot point of swinging lever motion. The light chain binding site is also boxed. Loop 1 and loop 2 of CCM are shorter than those of skeletal muscle myosin.

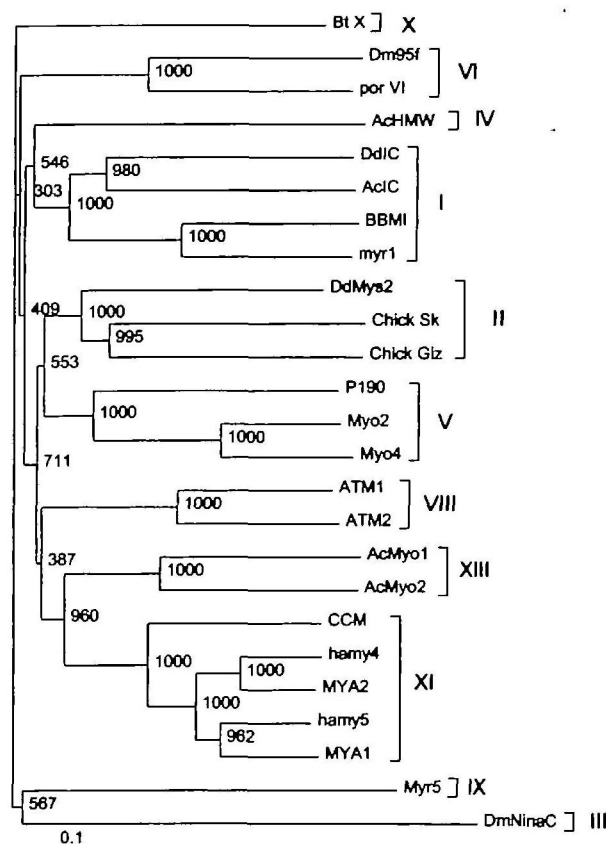


Fig. 3. An unrooted phylogenetic tree was generated using the neighbor-joining program Clustal X package. The sequence divergence between any pair of sequences is equal to the sum of the horizontal branch lengths connecting the two sequences. The bootstrap values at each node indicate the number of times out of 1,000 data resamplings that the sequences below a given node clustered together. The accession numbers are described below: Bt X, gb|U55042; Dm95f, sp|Q01989; por VI, pir|A54818; AcHMW, sp|P47808; DdIC, sp|P42522; AcIC, sp|P10569; BBMI, sp|P10568; myr1, pir|C45439; DdMys2, sp|P08799; Chick Sk, sp|P13538; Chick Glz, emb|X06546; P190, sp|Q02440; Myo2, sp|P19524; Myo4, sp|P32492; ATM1, emb|X69505; ATM2, emb|Z34292; AcMyo1, emb|U94397; AcMyo2, emb|U94398; CCM, emb|AB007459; hamy4, emb|U94789; hamy5, emb|U94785; MYA1, emb|Z28389; MYA2, emb|Z34293; Myr5, emb|X77609; NinaC, sp|P10676.

proteins (Fig. 4, lanes C and D). This band was also identical to that recognized by the antibody raised against biochemically purified characean myosin (Fig. 4, lane B).

Immunolocalization of characean myosin was done using an antibody against a coiled-coil region of this myosin heavy chain, because the sequence was quite unique. With appropriate caution to prevent non-specific binding of IgG to cytoplasmic components of characean cells, it was found that the antibody localized myosin on the bundles of actin filaments running parallel to the direction of streaming (data not shown).

Inhibition of Motile Activity by Antibody—An antibody against the head portion (amino acids 202 to 574) was raised and used to examine if the motile activity of characean myosin was impaired. When the myosin on a cover slip was treated with the antibody (0.35 mg/ml) for 15 min at room temperature, its motile activity was completely lost

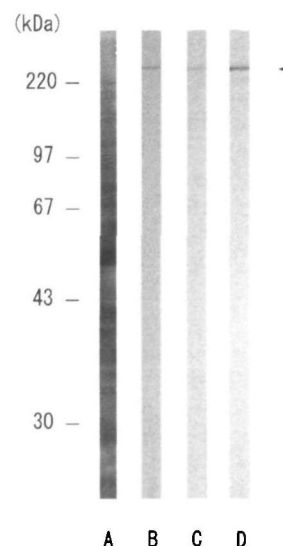


Fig. 4. Binding of *Chara corallina* myosin and antibodies raised against bacterially expressed peptides. Proteins were extracted from frozen and dried powder of *C. corallina* with SDS solution, run on 10% gel, and transferred to nitrocellulose membrane. Lane A shows protein bands stained with amido black. Lanes B to D show protein bands detected by antibodies against biochemically purified *C. corallina* myosin (B), antibodies against coiled-coil region peptide (C), and antibodies against distal tail domain peptide (D). All antibodies recognize the same protein band with a molecular mass of about 230 kDa (arrowhead).

(data not shown). An antibody against the globular tail-piece did not impair the motility.

DISCUSSION

The molecular weight and domain structure predicted from the sequence of this protein agreed very well with those of characean myosin purified biochemically and observed by electron microscopy. The molecular mass of the heavy chain estimated by SDS polyacrylamide gel electrophoresis was about 230 kDa (3), and the difference between this value and that determined in this study (247 723) is within experimental error in this high molecular mass range. Characean myosin observed by electron microscopy showed two heads, a relatively short rod portion, and a globular tail-piece (4). The presence of a central sequence that tends to form a coiled-coil structure indicates that this polypeptide can self-associate to form dimers. Together with the data of immunoblotting, immunolocalization, and the effect of antibody on the motile activity *in vitro*, these findings strongly suggest that the gene cloned in this study is that for the heavy chain of characean myosin, which drives the fast movement *in vivo* and *in vitro*.

Phylogenetic analysis suggests that characean myosin belongs to class XI. The role of class XI myosin in higher plant cells is not clear, but it seems to play a part in vesicle transport or cytoplasmic streaming, because its globular tail sequence has a similar motif to that of characean myosin, which is known to draw endoplasmic reticulum to generate streaming.

As mentioned earlier, the characean myosin supports very fast sliding movement of actin filaments. The aim of this study is to elucidate the mechanism of this movement

by comparing the primary structure of characean myosin with those of other slower myosins. The important components in the myosin motor domain that are deduced from the three-dimensional structure comparison of myosin, kinesin, Ras, and elongation factor Tu (12), are all preserved in this myosin. Amino acid sequences of a loop around a phosphate group (P-loop), switch I, switch II, and the helix following switch II are quite similar to those of muscle myosin (Fig. 2).

Definite differences were observed at the junctions between the 25- and 50-kDa domains (loop 1) and the 50- and 20-kDa domains (loop 2). These loops are known to be strikingly divergent among myosins. Loop 1 is close to the ATP binding site and, in the case of muscle myosin, ATP affects its susceptibility to various proteolytic enzymes (13). Change in this loop may alter the release rate of ADP and, therefore, the speed of the power stroke. Loop 2 of muscle myosin is protected from proteolysis by the binding of actin (14, 15) and can be cross-linked to the negatively charged amino-terminus of actin (16, 17). Cleavage of this loop lowers the affinity of muscle myosin to actin (18–20). Replacing this loop of *Dictyostelium* myosin with the corresponding loop of muscle myosin makes the actin-activated Mg ATPase activity of the chimera several-fold higher than that of the wild type (21). Loop 2 is important for the weak interaction with actin (19, 22). These two loops are very short in characean myosin compared to muscle myosin. The short loop 1 may increase the speed of the power stroke by facilitating the release of ADP during the interaction with actin. Tawada and Sekimoto suggested that the “weak interaction” may also have a profound effect on the sliding velocity by exerting a molecular drag force (23, 24). The sliding velocity is determined not simply by the speed of the power stroke. It is determined by the balance between the force generated by active heads and the velocity dependent drag force exerted by weakly interacting heads under one actin filament. If the drag force is low, then the final velocity will be high. The short and less positively charged loop 2 may confer the high translocating activity on characean myosin by reducing the weak interaction. Of course, the reason can not be so simple. Replacing these loops of *Dictyostelium* myosin with those of characean myosin will provide information about its high translocating activity. Study in this line is now in progress.

Characean cytoplasmic streaming is sensitive to SH reagents such as *N*-ethylmaleimide, and myosin was suggested to be the target of the reagent (25). The existence of cysteine residues at corresponding sites of reactive cysteine residues (SH₁ and SH₂) of muscle myosin supports the idea that the SH reagent stops the streaming by directly inactivating myosin.

The sequence showed six IQ motifs next to the head domain (Fig. 1). If this region is fully occupied by light chain or calmodulin, the head must be much larger than that of muscle myosin, which is the case in p190 (26). However, we did not observe such a long head by electron microscopy (4). The head size was similar to that of muscle myosin. It has been suggested that muscle myosin head changes shape in the presence of ATP or ADP (27). Since characean myosin was kept in a solution containing ATP during purification, we might have observed a kinked head.

The length of the coiled-coil region predicted from the sequence was much longer than that observed by electron

microscopy (90 vs. 50 nm). We noticed the same discrepancy in the case of class V myosin p190. The length of the coiled-coil region predicted from the sequence was about 53 nm (10) and that observed by electron microscopy was about 30 nm (26). These discrepancies can be explained if the globular tailpiece bends back toward the head.

The tailpiece of characean myosin also has a sequence motif conserved among class V and XI myosins (9, 10). The function of this conserved motif is not known, but it might play an important role in the interaction with membrane proteins, because it is conserved from animals to lower plants.

Further characterization of this unique myosin will help to expand our understanding not only about the mechanism of force generation but also about the regulation of intracellular transport of membranous structures.

We thank Dr. Y. Aoyama for the advice on immunoscreening. We also thank Drs E. Kamitsubo and M. Kikuyama for providing *Chara corallina*.

REFERENCES

1. Kacher, B. and Reese, T.S. (1988) The mechanism of cytoplasmic streaming in characean algal cells: sliding of endoplasmic reticulum along actin filaments. *J. Cell Biol.* **106**, 1545–1553
2. Shimmen, T. and Yokota, E. (1994) Physiological and biochemical aspects of cytoplasmic streaming. *Int. Rev. Cytol.* **155**, 97–139
3. Yamamoto, K., Kikuyama, M., Sutoh-Yamamoto, N., and Kamitsubo, E. (1994) Purification of actin based motor protein from *Chara corallina*. *Proc. Jpn. Acad.* **70**, 175–180
4. Yamamoto, K., Kikuyama, M., Sutoh-Yamamoto, N., Kamitsubo, E., and Katayama, E. (1995) Myosin from alga *Chara*: unique structure revealed by electron microscopy. *J. Mol. Biol.* **254**, 109–112
5. Sanger, F., Nicklen, S., and Coulson, A. (1977) DNA sequencing with chain-terminating inhibitors. *Proc. Natl. Acad. Sci. USA* **74**, 5463–5467
6. Lupas, A., Van Dyke, M., and Stock, J. (1991) Predicting coiled coils from protein sequences. *Science* **252**, 1162–1164
7. Lupas, A. (1996) Prediction and analysis of coiled-coil structures. *Methods Enzymol.* **266**, 513–525
8. Thompson, J.D., Gibson, T.J., Plewniak, F., Jeanmougin, F., and Higgins, D.G. (1997) The ClustalX windows interface: flexible strategies for multiple sequence alignment aided by quality analysis tools. *Nucleic Acids Res.* **24**, 4876–4882
9. Kinkema, M. and Schiefelbein, J. (1994) A myosin from a higher plant has structural similarities to class V myosins. *J. Mol. Biol.* **239**, 591–597
10. Espreafico, E.M., Cheney, R.E., Nascimento, A.A.C., Camilli, P.V.D., Larson, R.E., and Mooseker, M.S. (1992) Primary structure and cellular localization of chicken brain myosin-V (p190), an unconventional myosin with calmodulin light chains. *J. Cell Biol.* **119**, 1541–1557
11. Cope, M.J.T., Whisstock, J., Rayment, I., and Kendrick-Jones, J. (1996) Conservation within the myosin motor domain: implications for structure and function. *Structure* **4**, 969–987
12. Vale, R.D. (1996) Switches, latches, and amplifiers: common themes of G proteins and molecular motors. *J. Cell Biol.* **135**, 291–302
13. Yamamoto, K. (1989a) ATP-induced structural change in myosin subfragment-1 revealed by the location of protease cleavage sites on the primary structure. *J. Mol. Biol.* **209**, 703–709
14. Mornet, D., Pantel, P., Audemard, E., and Kassab, R. (1979) The limited tryptic cleavage of chymotryptic S-1: an approach to the characterization of the actin site in myosin heads. *Biochem. Biophys. Res. Commun.* **89**, 925–932
15. Yamamoto, K. and Sekine, T. (1979a) Interaction of myosin sub-

- fragment-1 with actin. I. Effect of actin binding on the susceptibility of subfragment-1 to trypsin. *J. Biochem.* **86**, 1855–1862
16. Sutoh, K. (1982) Identification of myosin-binding sites on the actin sequence. *Biochemistry* **21**, 3654–3661
 17. Yamamoto, K. (1989b) Binding manner of actin to the lysine-rich sequence of myosin subfragment 1 in the presence and absence of ATP. *Biochemistry* **28**, 5573–5577
 18. Yamamoto, K. and Sekine, T. (1979b) Interaction of myosin subfragment-1 with actin. III. Effect of cleavage of the subfragment-1 heavy chain on its interaction with actin. *J. Biochem.* **86**, 1869–1881
 19. Botts, J., Muhlrads, A., Takahashi, R., and Morales, M. F. (1982) Effects of tryptic digestion on myosin subfragment 1 and its actin-activated adenosinetriphosphatase. *Biochemistry* **21**, 6903–6905
 20. Yamamoto, K. (1991) Identification of the site important for the actin-activated MgATPase activity of myosin subfragment-1. *J. Mol. Biol.* **217**, 229–233
 21. Uyeda, T.Q.P., Ruppel, K.M., and Spudich, J.M. (1994) Enzymatic activities correlate with chimaeric substitutions at the actin-binding face of myosin. *Nature* **368**, 567–569
 22. DasGupta, G. and Reisler, E. (1989) Antibody against the amino terminus of α -actin inhibits actomyosin interactions in the presence of ATP. *J. Mol. Biol.* **207**, 833–836
 23. Tawada, K. and Sekimoto, K. (1991) Protein friction exerted by motor enzyme through a weak-binding interaction. *J. Theor. Biol.* **150**, 193–200
 24. Warshaw, D.M., Desrosiers, J.M., Work, S.S., and Trybus, K.M. (1990) Smooth muscle myosin cross-bridge interactions modulate actin filament sliding velocity *in vitro*. *J. Cell Biol.* **111**, 453–463
 25. Chen, J.C. and Kamiya, N. (1975) Localization of myosin in the internodal cell of *Nitella* as suggested by differential treatment with *N*-ethylmaleimide. *Cell Struct. Funct.* **1**, 1–9
 26. Cheney, R.E., O'Shea, M.K., Heuser, J.E., Coelho, M.V., Wolenski, J.S., Espreafico, E.M., Forscher, P., Larson, R.E., and Mooseker, M.S. (1993) Brain myosin-V is a two-headed unconventional myosin with motor activity. *Cell* **75**, 13–23
 27. Katayama, E. (1998) Quick-freeze deep-etch electron microscopy of the actin-heavy meromyosin complex during the *in vitro* motility assay. *J. Mol. Biol.* **278**, 349–367